

PACS numbers: 73.63.Nm, 74.78.Na, 75.30.Fv, 75.47.Lx, 75.60.Ej, 81.07.Vb, 85.35.Be

## Creating of Bounded Majorana Pairs in Superconducting Net of Quantum Nanowires in $\text{SmMnO}_{3+\delta}$

F. M. Bukhanko

*Donetsk Institute for Physics and Engineering named after O. O. Galkin,  
N.A.S. Ukraine,  
46, Nauky Ave.,  
03028 Kyiv, Ukraine*

In this work, the formation of a superconducting network of quantum nanowires in  $\text{SmMnO}_{3+\delta}$  manganites in two hidden topological states CSL1 and CSL2 of a chiral quantum spin liquid is experimentally studied. As believed, the states of bound pairs of Majorana fermions are trapped at the two ends of the quantum nanowire. The formation of nanofragments of 1D coupled charge and spin densities' waves with wave vectors  $\mathbf{q}_1 \parallel \mathbf{a}$  and  $\mathbf{q}_2 \parallel \mathbf{b}$  as regards directions in the crystal lattice within the magnetic fields  $H \geq 100$  Oe indicates formation in  $ab$  planes of 2D quantum-nanowires' net. Within the weak magnetic fields  $H = 100$  Oe, 350 Oe and 1 kOe, the continuous spectrum of the thermal excitations of bounded Majorana pairs in  $\text{SmMnO}_{3+\delta}$  in temperature interval of 4.2–12 K is divided into two low-energy Landau zones with numbers  $n = 1$  and  $n = 2$  with two specific features of magnetization  $M(T)$  in the shape of alternating double peaks and truncated Dirac cones.

У цій роботі експериментально вивчено утворення надпровідної сітки квантових нанопроводів у манганітах  $\text{SmMnO}_{3+\delta}$  у двох прихованих топологічних станах CSL1 і CSL2 кіральної квантової спінової рідини. Вважається, що стани пов'язаних пар Майоранових ферміонів захоплюються на двох кінцях квантового нанопроводу. Утворення нанофрагментів 1D-зв'язаних хвиль зарядової та спінової густин з хвильовими векторами  $\mathbf{q}_1 \parallel \mathbf{a}$  й  $\mathbf{q}_2 \parallel \mathbf{b}$  щодо напрямків кристалічної ґратниці у магнетних полях  $H \geq 100$  Е вказує на утворення в площинах  $ab$  2D-сітки квантових нанопроводів. У слабких магнетних полях  $H = 100$  Е, 350 Е і 1 кЕ безперервний спектр теплових збуджень пов'язаних Майоранових пар у  $\text{SmMnO}_{3+\delta}$  в інтервалі температур 4,2–12 К розбивається на дві низькоенергетичні зони Ландау з номерами  $n = 1$  і  $n = 2$  із двома особливостями намагнетованості  $M(T)$  у формі подвійних піків і зрізаних Діракових конусів, що чергуються.

**Key words:** Majorana and Dirac fermions, alternating double peaks and

truncated Dirac cones, chiral quantum spin liquid.

**Ключові слова:** Майоранові та Діракові ферміони, чергування подвійних піків і зрізаних Діракових конусів, кіральна квантова спінова рідина.

*(Received 24 September, 2024)*

## 1. INTRODUCTION

Topological superconductors (TS) in dimensions  $D = 1, 2$ , with broken time-reversal (TR) symmetry have recently attracted a lot of attention [1–10]. These systems support Majorana fermion excitations at order-parameter defects such as vortices and sample edges. Majorana fermion excitations, with second quantized operators  $\gamma$  satisfying the self-Hermitian condition  $\gamma^\dagger = \gamma$ , can be construed as quantum particles, which are their own antiparticles [11]. The self-Hermitian character of Majorana fermions (MFs) leads to a  $2D$  quasi-particle exchange statistics, which is non-Abelian [1, 12]. The non-Abelian statistics of MFs can be used as a robust quantum mechanical resource to implement fault-tolerant topological quantum computation (TQC) [13, 14]. In  $1D$  TS with broken TR symmetry, Majorana fermion modes are supposed to be trapped at the two ends of a quantum wire [13–15], which, in a  $2D$  quantum wire network [15], can potentially lead to successful demonstration of non-Abelian statistics as well as TQC [15–17]. According to Ref. [18], in flat-band superconductors, the group velocity  $v_F$  of charge carriers is extremely small, which leads to freezing of the kinetic energy. Superconductivity in this case seems impossible, since within the framework of the BCS theory this means the disappearance of such microproperties as the coherence length of Cooper pairs, their superfluidity rigidity, and the critical current. The authors report the existence of a group velocity of free charge carriers in the two-layer graphene studied by them, which is characteristic of a graphene superlattice with a Dirac superconducting flat zone [19–23]. For the filling factor of the moiré superlattice in superconducting graphene  $1/2 < \nu < 3/4$ , a very small value of the group velocity  $v_F \cong 1000$  m/sec was found. It is important to note that the measurement of superfluidity, which controls the electrodynamic response of a superconductor, shows that it is dominated not by kinetic energy, but by an interaction-controlled superconducting gap, which is consistent with the theories of the quantum geometric contribution [19–23]. Evidence has been found for the crossover of electron-pairs characteristic of BCS and Bose–Einstein condensation [24–27]. The superconducting properties of a deformed graphene, which in normal state has a spectrum of free charge carriers with a flat energy

band, were studied in Ref. [28].

According to Ref. [29], in systems with a condensed state, when a quasi-particle is a superposition of electron and hole excitations and its production operator  $\gamma^\dagger$  becomes identical to the annihilation operator  $\gamma$ , such a particle can be identified as a Majorana fermion. In the Reed–Green model, the Bogolyubov quasi-particles in the volume become dispersive Majorana fermions, and the bound state formed in the core of the vortex becomes the Majorana zero mode. The former is interesting as a new type of wandering quasi-particles, while the latter is useful as a qubit for topological quantum computing. In condensed matter, the constituent fermions are electrons. Because the electron has a negative charge, it cannot be a Majorana fermion. Nevertheless, Majorana fermions can exist as collective excitations of electrons. The resulting Majorana fermions do not retain the true Lorentz invariance of the Dirac equation, since they do not move at the speed of light. However, with proper length and time scaling, the resulting Majorana fermions also obey the Dirac equation. Such Majorana fermions appear within the boundaries of topological superconductors or in the class of spin-liquid systems [29].

The condensation of bosons in the form of a bound state of Majorana fermions was previously studied in topological superconductors by tunnelling spectroscopy [30–32]. The tunnelling conductivity spectra of topological superconductors depend on their size and symmetry. In one-dimensional topological superconductors with time reversal violation, there is an isolated single Majorana zero mode at each end. Tunnelling conductance due to the isolated zero mode shows a differential conductance peak  $dI/dV$  with zero offset height  $2e^2/h$  [30–32]. If one Majorana zero mode is coupled to another Majorana zero mode at the other end of the superconductor, the tunnelling conductance is highly dependent on the coupling  $t$  between the Majorana modes at the different ends. When the ratio  $t/\Gamma$  of the coupling between modes to the width of the fermion spectrum  $\Gamma$  is very small, the peak shape  $dI/dV$  is realized [32]. However, in the case of significant mixing of the two Majorana modes, the differential conductivity has the form of a trough. In this case, the zero-bias conductance vanishes. The cause of the coexistence of superconductivity and strong correlations in electron systems with flat bands was studied in Ref. [33]. Flat band systems with a low density of charge carrier states play an important role because the flat band energy range is so narrow that the Coulomb interactions between free carriers  $E_c \propto e^2/a$  dominate over the kinetic energy, which puts these materials in a regime with strong correlations. If the flat band is narrow in both energy and momentum, its occupation can be easily changed in a wide range from zero to full.

It is well known that Landau levels are a striking example of two-dimensional flat bands. They occur when a strong magnetic field acts on a 2D electron system. In this case, the electron motion is reduced by the Lorentz force to quantized cyclotron orbits. In this case, the translational degeneracy leads to completely flat zones, the width of which is completely determined by the degree of disorder. Partially filled Landau levels, first studied in semiconductor heterostructures, contain a rich set of competing orders, including ferromagnetism, charge-ordered band and bubble phases, and the best-known fractional quantum Hall liquids. The essential feature of these states is their intrinsic Berry curvature, which underlies their topological character and leads to integer and fractional quantum Hall effects. Twisted bilayer graphene has recently been found to exhibit highly correlated states and superconductivity. Thus, the formation of flat bands of Majorana fermions is a characteristic mechanism of topological superconductivity, BCS and Bose–Einstein condensation of bosons in the form of a bound state of 2D Majorana fermions and Dirac superconducting flat zone. The crossover of electron pairs characteristic of BCS and Bose–Einstein condensation of bosons in the form of a bound state of Majorana fermions (Majorana zero mode) was also studied in topological superconductors.

The phase transition of a quantum spin liquid (QSL) to a chiral state in 2D frustrated AFMs with different types of crystal lattice, caused by an external magnetic field close to  $H = 0$  Oe, has attracted great interest among theoreticians and experimenters [34, 35]. It was shown that the transition of the QSL to the chiral state induced by an external magnetic field is accompanied by a phase transition into a phase with a topological order and excitation of fractional fermions (Majorana fermions). Kitaev was the first to construct a quantitative model of the so-called  $Z_2$  quantum spin liquid (a spin liquid with a local  $Z_2$  magnetic flux in the unit cell) for spins  $S = 1/2$  located at the nodes of a quasi-two-dimensional hexagonal lattice [34]. As shown in work [35], the chiral spin liquid state spontaneously breaks time-reversal symmetry (TRS), but retains other symmetries. There are two topologically different CSL1 and CSL2 states of the chiral spin liquid separated by a quantum critical point. In this work, the formation of quantum nanowire-like net bounded Majorana pairs in  $\text{SmMnO}_{3+\delta}$  manganites was first experimentally studied in two hidden topological states CSL1 and CSL2 of chiral quantum spin liquid.

## 2. MATERIAL AND METHODS

Samples of self-doped manganites  $\text{SmMnO}_{3+\delta}$  ( $\delta \cong 0.1$ ) were obtained

from high-purity oxides of samarium and electrolytic manganese, taken in a stoichiometric ratio. The synthesized powder was pressed under pressure of 10 kbar into discs of 6 mm in diameter, 1.2 mm thick and sintered in air at a temperature of 1170°C for 20 h followed by cooling at a rate of 70°C/h. The resulting tablets were a single-phase ceramic according to x-ray data. X-ray studies were carried out with 300 K on DRON-1.5 diffractometer in radiation  $\text{NiK}_{\alpha_1+\alpha_2}$ . Symmetry and crystal lattice parameters were determined by the position and character splitting reflections of the pseudocubic perovskite-type lattice. Temperature dependences of  $dc$  magnetization were measured using a VSM EGG (Princeton Applied Research) vibrating magnetometer and a nonindustrial magnetometer in ZFC and FC modes.

### 3. RESULTS AND DISCUSSION

According to our previous work [36], the temperature dependences of the magnetization of frustrated manganites  $\text{La}_{1-y}\text{Sm}_y\text{MnO}_{3+\delta}$  ( $\delta \cong 0.1$ ,  $y = 0.85, 1.0$ ) contain two sharp peaks  $M(T)$  of different intensity at close temperatures  $T_1$  and  $T_2$  slightly above the critical temperature  $T_c$  of the phase transition of the samples to the coherent superconducting state. It was shown that these features correspond to the Lindhard divergence  $\chi_L(\mathbf{q}_{nest})$  of the temperature dependence of the paramagnetic susceptibility of stripe-like 1D electron/spin correlations modulated with the wave vectors  $\mathbf{q}_{nest1} = 2\mathbf{k}_{F1}$  and  $\mathbf{q}_{nest2} = 2\mathbf{k}_{F2}$ . The appearance and evolution of the magnetization features with increasing field are explained by the formation in  $ab$  planes with complete nesting of the electron-hole regions of the Fermi surface of a spatial modulation of the electronic and magnetic properties in the form of fragments of two fluctuating quasi-one-dimensional waves of the charge/spin density (CDW/CDW) incommensurate with the crystal lattice with the wave vectors  $\mathbf{q}_1 \parallel \mathbf{a}$  and  $\mathbf{q}_2 \parallel \mathbf{b}$  directions. As can be seen in Fig. 1, the peak features of the magnetization  $M(T)$  in  $\text{SmMnO}_{3+\delta}$  arise at temperatures  $T_1 = 20$  K and  $T_2 = 50$  K slightly above  $T_c = 12$  K. In contrast to the sample with  $y = 0.85$ , the intensity of the peak feature near the temperature  $T_1$  in  $\text{SmMnO}_{3+\delta}$  is negligible but finite. A small Curie-like increase in magnetization at  $T \rightarrow 0$  K should also be noted. An increase in the measuring field strength to 350 Oe did not lead to a qualitative change in the temperature dependence of magnetization.

Cardinal changes in the magnetization  $M(T)$  were detected during measurements in a magnetic field of  $H = 1$  kOe. An increase in the magnetic field led to a decrease in the Kosterlitz–Thouless jump in the magnetization of the sample near the temperature  $T_c = 12$  K of its transition to the coherent SC state, complete suppression of the

magnetization peak near  $T_1$  and significant broadening of the  $M(T)$  peak near  $T_2$ .

The final stage of the evolution of the temperature dependences of magnetization  $M(T)$  in  $\text{SmMnO}_{3+\delta}$  with increasing external magnetic field strength can be considered the results of measurements in a field of  $H = 3.5$  kOe, shown in Fig. 2.

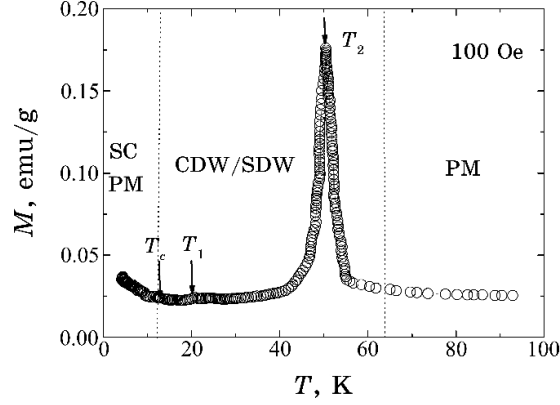


**Fig. 1.** Temperature dependence of magnetization  $M(T)$  in a field  $H = 100$  Oe in the ZFC-measurement mode. In the ZFC mode of magnetization measuring in the temperature range  $4.2 \leq T \leq 100$  K, a coherent superconducting state with a critical temperature  $T_c = 12$  K is observed. In the temperature range 12–60 K, the charge/spin density wave state is realized in the form of a two-peak magnetization feature  $M(T)$ .

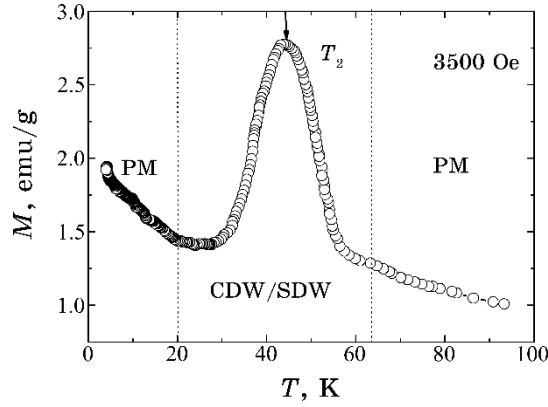


**Fig. 2.** Temperature dependence of magnetization  $M(T)$  in a field  $H = 3500$  Oe in the ZFC-measurement mode in the temperature range  $4.2 \leq T \leq 100$  K. A coherent superconducting state with a critical temperature  $T_c = 12$  K is absent. In the temperature range 20–70 K, the spin-density wave state is realized in the form of a wide-peak magnetization feature  $M(T)$ .

At temperatures below 60 K of the transition of the sample from the paramagnetic phase to the phase with periodic nanoscale ordering of quasi-particles in the form of fluctuating CDW/CDW fragments, only a wide peak of magnetization near the temperature  $T_2 \approx 42$  K is preserved. As a result of the increase in the external magnetic field strength in the range of fields of  $100 \text{ Oe} \leq H \leq 3500 \text{ Oe}$ , a ‘metallic’ state of the SDW type with a fairly high density of free quasi-particles at the Fermi level was formed in the  $\text{SmMnO}_{3+\delta}$  sample at temperatures below 60 K. This indicates a small value (absence) of the charge pseudogap in the electron spectrum of charge/spin carriers in  $\text{SmMnO}_{3+\delta}$  at  $EF$  in a magnetic field of  $H = 3.5 \text{ kOe}$ .

Thus, an increase in the field strength to  $H = 3.5 \text{ kOe}$  led to the suppression of the charge pseudogap in the quasi-particle spectrum, to a decrease in the 1D CDW amplitude and, accordingly, to an increase in the amplitude of the fluctuating 1D SDW incommensurate with the crystal lattice. With increasing  $H$ , we have a transformation of the mixed state of nanofragments of charge-spin density waves into a 1D spin-density wave. The increase in the width of the  $M(T)$  peak near  $T_2$  with increasing  $H$  is apparently caused by the renormalization of the spectrum by coupling with magnons. Thus, we associate the appearance of the two peak features of magnetization at temperatures slightly above  $T_c$  with the formation in  $\text{SmMnO}_{3+\delta}$  in weak fields  $H \geq 100 \text{ Oe}$  of nanofragments of 1D coupled charge and spin density waves incommensurate with the crystal lattice in two spatially separated regions of the sample (conventionally ‘metallic’ and ‘dielectric’ nanophases) with high and low densities of states free carriers at the Fermi level  $N_1(E_F) \ll N_2(E_F)$ . With an increase in the external magnetic field strength  $H$ , ‘metallization’ of the spectrum of free charge carriers in  $\text{SmMnO}_{3+\delta}$  occurs.

Previously, the formation of a broad continuum of spinon pair excitations in  $\text{SmMnO}_{3+\delta}$  in the ‘weak magnetic field’ regime  $H = 100 \text{ Oe}$ ,  $1 \text{ kOe}$  in the FC mode is explained in the framework of the Landau quantization models of the compressible spinon gas with fractional values of the factor  $\nu$  of filling three overlapping bands with quantum numbers  $n = 1, 2$ , and  $3$  [37]. In the regime of ‘strong magnetic field’  $H = 3.5 \text{ kOe}$ , the new step-like quantum oscillations of temperature dependences of supermagnetization of incompressible spinon liquid were found. According to the experimental results obtained in this work, in low-energy Landau zones with numbers  $n = 1, 2$ , with an increase in the strength of the measuring field  $H$ , two alternating supermagnetization features are formed, which are characteristic of the excitation of 2D Majorana and Dirac fermions.

A singularity of supermagnetization  $M(T)$  in Landau band with number  $n = 1$  in a magnetic field  $H = 100 \text{ Oe}$  has a double-peaks’ shape with a strong dip near the average temperature  $T \cong 4.65 \text{ K}$  (Fig. 3).

However, in the zone with  $n = 2$ , the singularity has a distinct shape: a truncated Dirac cone with a flat top in an ultra-narrow energy range  $\Delta E \cong 0.01$  meV with a weak dip in its top near the average excitation temperature of massless Dirac quasi-particles,  $T \cong 5.41$  K (Fig. 4).

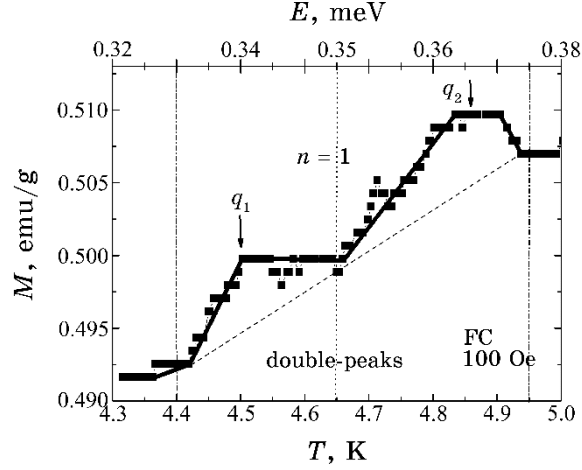


**Fig. 3.** An alternate excitation in the FC-measurement mode of a double-peaks' feature in the magnetic response arise from excitation of bounded Majorana pairs in Landau zone with  $n = 1$  near average temperature  $T \cong 4.65$  K in external magnetic field  $H = 100$  Oe (CSL1 state).

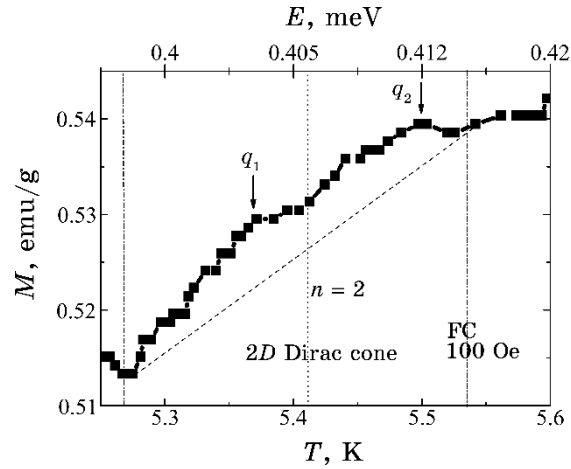


**Fig. 4.** An alternate excitation in the FC-measurement mode of a 2D Dirac cones-like feature in the magnetic response arise from excitation of bounded Majorana zero modes with energy  $E_{MZM} \cong 0.4$  meV in Landau zone with  $n = 2$  in external magnetic field  $H = 100$  Oe (CSL2 state).



In a magnetic field  $H = 350$  Oe, the alternation of magnetization features  $M(T)$  in the zones with number  $n = 1$  and 2 changed to the opposite. In the zone with number  $n = 1$ , a singularity  $M(T)$  in Landau band has a shape a truncated Dirac cone with a flat top in a wider energy range  $\Delta E \cong 0.05$  meV with a weak dip in its top near the average excitation temperature of massless Dirac quasi-particles  $T \cong 4.6$  K. At the same time, in the zone  $n = 2$ , the supermagnetization feature has the form of two broad weak peaks  $M(T)$  with a strong dip near the average temperature of the excitation of Majorana fermions near  $T \cong 5.5$  K. As can be seen in Figs. 5, 6, this regularity in the alternation of features  $M(T)$  in low-energy Landau bands with number  $n = 1$  and 2 is also preserved in the measuring field  $H = 1$  kOe despite a significant expansion of features  $M(T)$  caused by the appearance of strong fluctuations of the topological order in spin system.

In the  $n = 1$  zone, a two-peak super magnetization feature forms near the average temperature  $T \cong 4.6$  K, while in the  $n = 2$  zone, with increasing temperature near the average excitation temperature  $T \cong 5.5$  K, a cone-like feature  $M(T)$  with a flat top appears in a wide energy range  $\Delta E \cong 0.05$  meV. Thus, an increase in the magnetic field strength in  $\text{SmMnO}_{3+\delta}$  in the ‘weak magnetic fields’ mode is accompanied by a rearrangement of singularities of super magnetization in low-energy Landau bands with number  $n = 1$  and 2. As shown in Fig. 7, new step-like features of super magnetization form in ‘strong magnetic fields’ regime. An alternate permutation of the

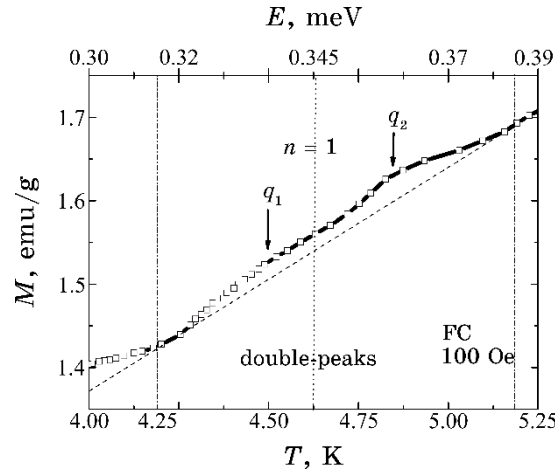


**Fig. 5.** An alternate excitation in the FC-measurement mode of a double-peaks’ feature in the magnetic response arise from excitation of bounded Majorana pairs in Landau zone with  $n = 1$  near average temperature  $T \cong 4.65$  K in external magnetic field  $H = 1$  kOe (CSL1 state).

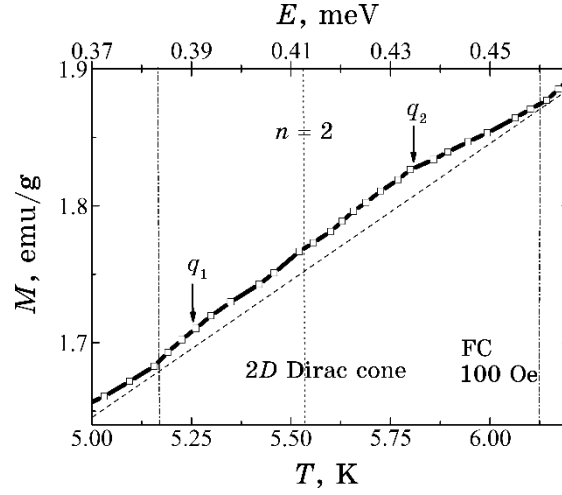


**Fig. 6.** An alternate excitation in the FC-measurement mode of a Dirac cones-like feature in the magnetic response arise from excitation of bounded Majorana modes with energy  $E_{MZM} \cong 0.41$  meV in Landau zone with  $n = 2$  near average temperature  $T \cong 5.5$  K in external magnetic field  $H = 1$  kOe (CSL2 state).

double-peaks' and truncated-Dirac-cones' features of the magnetization  $M(T)$  in two Landau bands with number  $n = 1, 2$  during the Landau quantization of the fermion pairs spectrum in  $\text{SmMnO}_{3+\delta}$  in 'weak magnetic fields' regime may be explained by the existence in this material of two well-known in the literature hidden states CSL1 and CSL2 of the chiral spin liquid.

#### 4. CONCLUSIONS

According to the experimental results of this work, the temperature dependences of the magnetization of  $\text{SmMnO}_{3+\delta}$  in ZFC-measurement mode contain two sharp peaks of different intensity at close temperatures  $T_1$  and  $T_2$  slightly above the critical temperature  $T_c$  of the phase transition of the samples to the coherent superconducting state.

It was shown that these features correspond to the Lindhard divergence  $\chi_L(\mathbf{q}_{nest})$  of the temperature dependence of the paramagnetic susceptibility of stripe-like 1D electron/spin correlations modulated with the wave vectors  $\mathbf{q}_{nest1} = 2\mathbf{k}_{F1}$ ,  $\mathbf{q}_{nest2} = 2\mathbf{k}_{F2}$ . We associate the appearance of the two-peak features of magnetization with the formation in  $\text{SmMnO}_{3+\delta}$  in weak fields  $H \geq 100$  Oe of nanofragments of 1D coupled charge and spin density waves incommensurate with the crystal lattice in two spatially separated regions of the

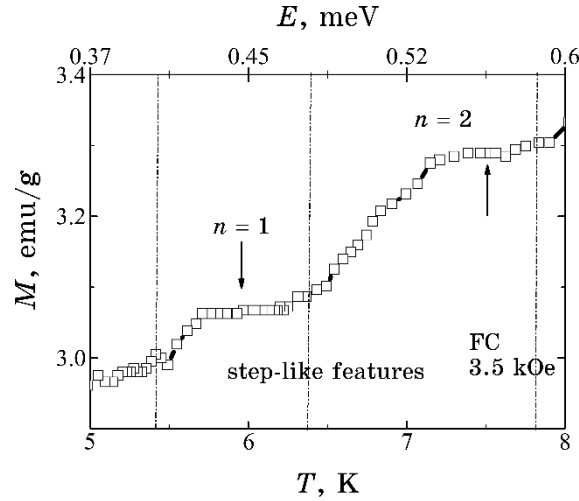


Fig. 7. The thermal excitation in the FC-measurement mode of a step-like features of temperature dependence of supermagnetization in interval temperature 5–8 K of incompressible quantum spin liquid in Landau zones with  $n = 1$  and  $2$  in external magnetic field  $H = 3.5$  kOe.

sample (conventionally ‘metallic’ and ‘dielectric’ nanophases) with high and low densities of states free carriers at the Fermi level  $N_1(E_F) \ll N_2(E_F)$ . An increase in the field strength to  $H = 3.5$  kOe led to: 1) the suppression of the charge pseudogap in the quasiparticle spectrum; 2) a decrease in the 1D CDW amplitude; 3) an increase in the amplitude of the fluctuating 1D SDW incommensurate with the crystal lattice. With increasing  $H$ , we have a transformation of the mixed state of nanofragments of 1D CDW/SDW into a 1D SDW.

In the weak magnetic fields  $H = 100$  Oe, 350 Oe and 1 kOe, the continuous spectrum of the thermal excitations of bounded Majorana pairs in  $\text{SmMnO}_{3+\delta}$  in interval temperature 4.2–12 K in FC mode is divided into two low-energy Landau zones with numbers  $n = 1$ ,  $n = 2$ , with two specific features of magnetization  $M(T)$  in the shape of alternating double peaks and truncated Dirac cones. An increase in the magnetic field strength in  $\text{SmMnO}_{3+\delta}$  to  $H = 3.5$  kOe is accompanied by a rearrangement of singularities of super magnetization in low-energy Landau bands with number  $n = 1$  and  $2$ : new step-like features of super magnetization form in ‘strong magnetic fields’ regime. An alternate permutation of the double-peaks’ and truncated-Dirac-cones’ features of the magnetization  $M(T)$  in two Landau bands with number  $n = 1, 2$  during the Landau quantization of the bounded Majorana pairs spectrum in  $\text{SmMnO}_{3+\delta}$  in ‘weak magnetic fields’ regime may be explained by the existence in

this material of two well-known in the literature hidden states CSL1 and CSL2 of the chiral spin liquid.

## REFERENCES

1. N. Read and D. Green, *Phys. Rev. B*, **61**, Iss. 15: 10267 (2000); <https://doi.org/10.1103/PhysRevB.61.10267>
2. J. D. Sau, R. M. Lutchyn, S. Tewari, and S. Das Sarma, *Phys. Rev. Lett.*, **104**, Iss. 4: 040502 (2010); <https://doi.org/10.1103/PhysRevLett.104.040502>
3. J. D. Sau, S. R. Tewari, R. M. Lutchyn, T. D. Stanescu, and S. Das Sarma, *Phys. Rev. B*, **82**, Iss. 21: 214509 (2010); <https://doi.org/10.1103/PhysRevB.82.214509>
4. M. Leijnse and K. Flensberg, *arXiv:1107.5703v2* [cond-mat.supr-con] 30 Nov 2011.
5. Y. Oreg, G. Refael, and F. V. Oppen, *Phys. Rev. Lett.*, **105**, Iss. 17: 177002 (2010); <https://doi.org/10.1103/PhysRevLett.105.177002>
6. S. Tewari and J. D. Sau, *Phys. Rev. Lett.*, **109**, Iss. 15: 150408 (2012); <https://doi.org/10.1103/PhysRevLett.109.150408>
7. J. D. Sau, S. Tewari, and S. Das Sarma, *arXiv:1111.2054v3* [cond-mat.supr-con] 27 Feb 2012.
8. T. P. Choy, J. M. Edge, J. M. Akhmerov, and C. W. J. Beenakker, *arXiv:1108.0419v1* [cond-mat.mes-hall] 1 Aug 2011.
9. I. Martin and A. F. Morpurgo, *arXiv:1110.5637v2* [cond-mat.mes-hall] 29 Mar 2012.
10. W. DeGottardi and D. Sen, *arXiv:1208.0015v1* [cond-mat.str-el] 31 Jul 2012.
11. F. Wilczek, *Nature Phys.*, **5**, Iss. 5: 614 (2009); <https://doi.org/10.1038/nphys1380>
12. K. Pakrouski, M. R. Peterson, T. Jolicoeur, V. W. Scarola, C. Nayak, and M. Troyer, *Phys. Rev. X*, **5**, Iss. 4: 021004 (2015); [doi:10.1103/PhysRevX.5.021004](https://doi.org/10.1103/PhysRevX.5.021004)
13. A. Kitaev, *Ann. Phys.*, **303**, Iss. 1: 2 (2003); [https://doi.org/10.1016/S0003-4916\(02\)00018-0](https://doi.org/10.1016/S0003-4916(02)00018-0)
14. C. Nayak, S. H. Simon, A. Stern, M. Freedman, and S. Das Sarma, *Rev. Mod. Phys.*, **80**, Iss. 3: 1083 (2008); <https://doi.org/10.1103/RevModPhys.80.1083>
15. J. Alicea, Y. Oreg, G. Refael, F. von Oppen, and M. P. A. Fisher, *Nature Physics*, **7**, Iss. 2: 412 (2011); <http://dx.doi.org/10.1038/nphys1915>
16. J. D. Sau, S. Tewari, R. Lutchyn, T. Stanescu, and S. Das Sarma, *arXiv:1006.2829v2* [cond-mat.supr-con] 30 Jun 2010.
17. R. M. Lutchyn, T. D. Stanescu, and S. Das Sarm, *Phys. Rev. Lett.*, **106**, Iss. 12: 127001 (2011); <https://doi.org/10.1103/PhysRevLett.106.127001>
18. H. Tian, S. Che, T. Xu, P. Cheung, K. Watanabe, T. Taniguchi, M. Randeria, F. Zhang, C. N. Lau, and M. W. Bockrath, *arXiv 2112.13401* [cond-mat.supr-cond] 2021.
19. S. Peotta and P. Törmä, *arXiv:1506.02815v3* [cond-mat.supr-con] 2 Dec 2015.

20. X. Hu, T. Hyart, D. I. Pikulin, and E. Rossi, *Phys. Rev. Lett.*, **123**, Iss. 23: 237002 (2019); <https://doi.org/10.1103/PhysRevLett.123.237002>
21. F. Xie, Z. Song, B. Lian, and B. A. Bernevig, *Phys. Rev. Lett.*, **124**, Iss. 16: 167002 (2020); <https://doi.org/10.1103/PhysRevLett.124.167002>
22. A. Julku, T. J. Peltonen, L. Liang, T. T. Heikkilä, and P. Törmä, *Phys. Rev. B*, **101**, Iss. 6: 060505 (2020); <https://doi.org/10.1103/PhysRevB.101.060505>
23. N. Verma, T. Hazra, and M. Randeria, *Proc. Nat. Acad. Sci.*, **118**, Iss. 8: e2106744118 (2021); <https://doi.org/10.1073/pnas.2106744118>
24. Q. Chen, J. Stajic, S. Tan, and K. Levin, *Physics Reports*, **412**, Iss. 1: 1 (2005); <https://doi.org/10.1016/j.physrep.2005.02.005>
25. M. Randeria and E. Taylor, *Annual Reviews of Condensed Matter Physics*, **5**, Iss. 3: 209 (2014); <https://doi.org/10.1146/annurev-conmatphys-031113-1338299>
26. Y. Nakagawa, Y. Kasahara, T. Nomoto, R. Arita, T. Nojima, and Y. Iwasa, *Science*, **372**, Iss. 4: 190 (2021); [doi:10.1126/science.abb9860](https://doi.org/10.1126/science.abb9860)
27. T. T. Heikkilä and G. E. Volovik, *Basic Physics of Functionalized Graphite*, **123**, Iss. 7: 123 (2016); [https://doi.org/10.1007/978-3-319-39355-1\\_6](https://doi.org/10.1007/978-3-319-39355-1_6)
28. V. J. Kauppila, F. Aikebaier, and T. T. Heikkilä, *Phys. Rev. B*, **93**, Iss. 6: 214505 (2016); <https://doi.org/10.1103/PhysRevB.93.214505>
29. M. Sato and Y. Ando, *Rep. Prog. Phys.*, **80**, Iss. 7: 076501 (2017); <https://doi.org/10.1088/1361-6633/aa6ac7>
30. K. T. Law, P. A. Lee, and T. K. Ng, *Phys. Rev. Lett.*, **103**, Iss. 23: 237001 (2009); <https://doi.org/10.1103/PhysRevLett.103.237001>
31. K. Flensberg, *Phys. Rev. B*, **82**, Iss. 18: 180516 (2010); <https://doi.org/10.1103/PhysRevB.82.180516>
32. P. A. Ioselevich and M. V. Feigel'man, *New J. Phys.*, **15**, Iss. 5: 055011 (2013); <https://doi.org/10.1088/1367-2630/15/5/055011>
33. L. Balents, C. R. Dean, D. K. Efetov, and A. F. Young, *Nature Physics*, **16**, Iss. 5: 725 (2020); <https://doi.org/10.1038/s41567-020-0906-9>
34. A. Kitaev, *Annals of Physics*, **321**, Iss. 6: 2 (2006); <https://doi.org/10.1016/j.aop.2005.10.005>
35. H. Yao and S. A. Kivelson, *Phys. Rev. Lett.*, **99**, Iss. 24: 247203 (2007); <https://doi.org/10.1103/PhysRevLett.99.247203>
36. F. N. Bukhanko and A. F. Bukhanko, *Physics of the Solid State*, **61**, Iss. 12: 2525 (2019); [doi:10.1134/S1063783419120084](https://doi.org/10.1134/S1063783419120084)
37. F. N. Bukhanko and A. F. Bukhanko, *Fiz. Nizk. Temp.*, **47**, Iss. 11: 1021 (2021); [doi:10.1063/10.0006569](https://doi.org/10.1063/10.0006569)